CHEMISTRY
A EUROPEAN JOURNAL

DOI: 10.1002/chem.200700655

VIP Bis-alkynyl Diruthenium Compounds with Built-in Electronic Asymmetry: Toward an Organometallic Aviram–Ratner Diode

Jie-Wen Ying, Antoinette Cordova, Tony Y. Ren, Guo-Lin Xu, and Tong Ren*[a]

Abstract: Conditions to prepare *trans*-$[Ru_2(dmba)_4(C{\equiv}CAr)_2]$ from $[Ru_2(dmba)_4(NO_3)_2]$ (DMBA = *N*,*N*′-dimethylbenzamidinate) and $HC{\equiv}CAr$ were optimized; Et_2NH was found to be the most effective among a number of weak bases in facilitating the product formation. Furthermore, a series of unsymmetric *trans*-$[(ArC{\equiv}C)Ru_2(dmba)_4(C{\equiv}CAr')]$ compounds were prepared under optimized conditions, in which one or both of Ar and Ar′ are donor (NMe_2)-/acceptor (NO_2)-substituted phenyls. While the X-ray crystallographic studies revealed a minimal structural effect upon donor/acceptor substitution, voltammetric measurements indicated a significant influence of substituents on the energy level of frontier orbitals. In particular, placing a donor and an acceptor on the opposite ends of *trans*-$[(ArC{\equiv}C)Ru_2(dmba)_4(C{\equiv}CAr')]$ moiety results in an energetic alignment of frontier orbitals that favors a directional electron flow, a necessary condition for unimolecular rectification.

Keywords: alkyne ligands · electronic asymmetry · molecular diodes · ruthenium

Introduction

Three decades have passed since the publication of the seminal proposal of molecular rectification based on the donor–(saturated bridge)–acceptor (D-σ-A) assembly by Aviram and Ratner (AR Ansatz).[1] This proposal ushered in the era of molecular electronics, during which many prototypes of molecular electronic devices have been realized.[2] Early demonstrations of electrical rectifications by both the donor–(π-bridge)–acceptor (D-π-A) and D-σ-A were based on the measurements on LB films.[3,4] Diode-like behavior was reported for the SAMs (self assembled monolayer) of thiophene–thiazole diblock oligomers,[5] in which the donor and acceptor segments are directly bonded. Single-molecule rectifications have been documented recently based on the STM studies of azafullerene ($C_{59}N$)[6] and substituted graphenes,[7] and the mechanically controlled break junction measurement of an unsymmetrical oligo(phenylene ethynylene).[8] Notably, all of the above-mentioned studies were based on organic donor–bridge–acceptor diads.

There has been intense interest in the use of inorganic–organic hybrid molecules as both molecular wires and other active components of molecular electronic devices.[9,10] Notably, prototypes of single-molecule transistor have been realized based on mono-,[11] di-,[12] and trimetallic complexes.[13] In a broader scope, facile electron/hole transfer within metal–σ-alkynyl scaffolds have been demonstrated in bulk with metal centers including Fe,[14] Re,[15] Fe/Re,[16] Mn,[17] and Ru,[18] revealing the potential of metal–σ-alkynyl molecules in molecular electronics. Further demonstrating the potential of organometallics in molecular electronics, a recent report revealed that $[HS(C_6H_4C{\equiv}C)_2\text{-}Fc\text{-}(C{\equiv}CC_6H_4)_2SH]$ exhibits the near quantum conductance, which is two orders of magnitude higher than that of the corresponding OPE (OPE = oligo(phenyleneethynylene)) without ferrocene, namely $HS(C_6H_4C{\equiv}C)_4(C_6H_4)SH$.[19] We are interested in the synthesis of linear conjugated molecules based on alkynyl adducts on a diruthenium paddlewheel core, and their utility as the active species in molecular electronic devices.[20] Voltammetric and spectroelectrochemical data obtained for these compounds indicate facile charge delocalization across both the carbon-rich bridges and the diruthenium units.[21–23] Demonstrating the promise of Ru_2–alkynyl species as molecular wires, STM (scanning tunneling microscopy) studies of $[Ru_2(ap)_4\text{-}\sigma\text{-}(C{\equiv}CC_6H_4)_2S-]$ embedded in an alkane thiol matrix revealed a significantly improved molecular conductance relative to that of an OPE of similar length.[24]

Previously, we reported a series of symmetrical $[Ru_2(dmba)_4(C{\equiv}CAr)_2]$ compounds, in which DMBA is *N*,*N*′-di-

---

[a] Dr. J.-W. Ying, A. Cordova, T. Y. Ren, Dr. G.-L. Xu, Prof. T. Ren
Department of Chemistry, Purdue University
West Lafayette, IN 47907 (USA)
Fax (+1) 765-494-0239
E-mail: tren@purdue.edu

methylbenzamidinate and Ar is phenyl bearing electron donor or acceptor substituent; the influence of these substituents on the electronic properties of these diruthenium species were investigated.[25] In this contribution, we describe the synthesis of both symmetric [$Ru_2(dmba)_4(C{\equiv}CAr)_2$] (**1**–**3**) and unsymmetric [$(ArC{\equiv}C)Ru_2(dmba)_4(C{\equiv}CAr')$] type compounds (**4**–**7**), and the electronic asymmetry in the latter type of compounds that may render the function of single-molecule rectifier.

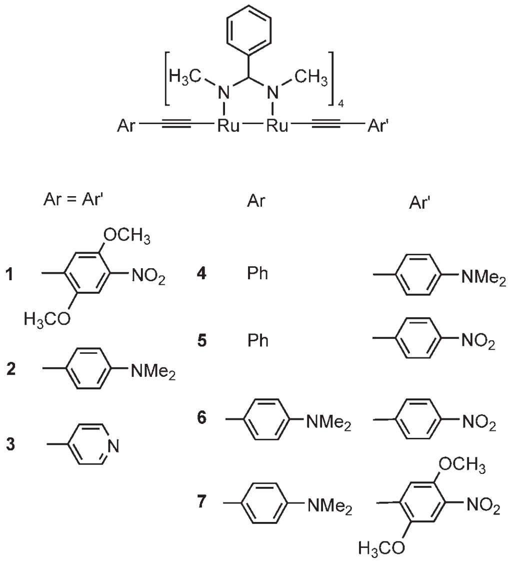

Results and Discussion

Synthesis: During the early studies of symmetric [$Ru_2(dmba)_4(C{\equiv}CY)_2$]-type compounds (Y = aryl or SiR_3), the bis-alkynyl species was obtained from the anion metathesis reaction between [$Ru_2(dmba)_4Cl_2$] and $LiC{\equiv}CY$.[26,27] It was soon discovered that [$Ru_2(dmba)_4X_2$] (X = NO_3 or BF_4) reacts with an unactivated alkyne $HC{\equiv}CR$ in the presence of Et_3N at room temperature and in an ambient atmosphere.[25,28] The use of unactivated alkyne proved to be advantageous in the high yield synthesis of compounds containing strong electrophilic functional groups, such as NO_2 and CN, and the insensitivity of the reaction toward air/moisture enabled easy monitoring of reaction progress. However, the original protocol had shortcomings, including the use of terminal acetylenes in large excess (>5 equiv) and extended reaction time (overnight). To further improve this reaction, efforts were focused on searching for organic bases as the substitute of triethylamine. The reaction between [$Ru_2(dmba)_4(NO_3)_2$] and phenylacetylene was utilized as the benchmark reaction for the screening. As shown by the data in Table 1, use of Et_2NH resulted in the fastest consumption of [$Ru_2(dmba)_4(NO_3)_2$], while reactions with bulkier bases required significantly longer reaction times.

Under the optimized conditions, new symmetric [$Ru_2(dmba)_4(C{\equiv}CAr)_2$] compounds were successfully prepared with Ar as 2,5-dimethoxy −4-nitrophenyl (**1**), 4-dimethylaminophenyl (**2**), and 4-pyridyl (**3**). Compound **3** was also prepared from the reaction between [$Ru_2(dmba)_4(NO_3)_2$] and 4-ethynylpyridine hydrochloride in the presence of either potassium *tert*-butoxide or Et_2NH.

Table 1. Base dependence of alkynylation reactions.[a]

	Et_2NH	$i$$Pr_2NH$	Et_3N	$i$$Pr_2EtN$
HC_2Ph	2 equiv	2 equiv	2 equiv	2 equiv
[$Ru_2(dmba)_4(NO_3)_2$]	1 equiv	1 equiv	1 equiv	1 equiv
reaction time [h]	1	3	18	30

[a] Conditions: 0.01 mmol [$Ru_2(dmba)_4(NO_3)_2$], 0.1 mmol of base, 5 mL of THF, 25 °C. Progress of the reaction was monitored by TLC (solvent: THF/hexane = 1:2, v/v).

The synthesis of an unsymmetrical compound [$(FcC{\equiv}C)Ru_2(dmba)_4(C{\equiv}C\text{-}C{\equiv}CFc)$] was accomplished recently in our laboratory,[21] for which [$Ru_2(dmba)_4Cl_2$] was treated with a mixture of $LiC{\equiv}CFc$ and $LiC{\equiv}C\text{-}C{\equiv}CFc$; the desired unsymmetrical compound was separated from the symmetric by-products by column chromatography. This approach could be problematic for the preparation of compounds such as *trans*-[$(4\text{-}NO_2PhC{\equiv}C)Ru_2(dmba)_4(C{\equiv}CPh\text{-}4\text{-}NMe_2)$] (**6**), because of the potential interaction between *n*-BuLi and the nitro group.[25] On the other hand, the weak base protocol is compatible with electrophilic functional groups and appears ideal for the synthesis of compound **6**. Thus, the reaction between [$Ru_2(dmba)_4(NO_3)_2$] and a mixture of $4\text{-}Me_2NC_6H_4C{\equiv}CH$ and $4\text{-}O_2N\text{-}C_6H_4C{\equiv}CH$ in the presence of diethyl amine yielded three products as indicated in Scheme 1. The distribution of the three products was dependent on the ratio of two acetylenes, and a 1:3 molar ratio of $4\text{-}Me_2NC_6H_4C{\equiv}CH$ and $4\text{-}O_2N\text{-}C_6H_4C{\equiv}CH$ was found to be optimal for the maximum yield of compound **6**. Attempts to separate **6** from two symmetric compounds, however, were hampered by both the poor solubility and similarity in polarity of three compounds. To overcome these problems, a modified ligand 2,5-dimethoxy-4-nitrophenylethyne was invoked and the presence of methoxy substituents greatly improved the solubility.[29,30] Thus, the reaction of [$Ru_2(dmba)_4(NO_3)_2$], $4\text{-}Me_2NC_6H_4C{\equiv}CH$, and the new acetylene resulted in a mixture of compounds **1**, **2**, and **7**, and the desired compound **7** was separated from the symmetrical compounds **1** and **2** by silica column chromatography in a yield of 26%. Other unsymmetric compounds **4** and **5** were similarly prepared and purified in moderate yields.

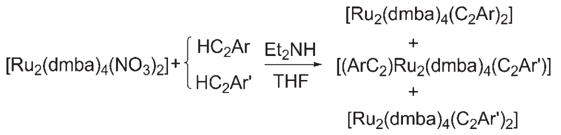

Scheme 1.

Aryleneethynyls ($ArC{\equiv}C$-) are the most common ligands for metal–alkynyl compounds.[9,31,32] While hundreds of structural examples of bis-aryleneethynyl compounds can be found in the Cambridge Structure Database, asymmetric compounds of the *trans*-[ArC≡C-(ML$_n$)-C≡CAr′]-type are rare.[33–35] These asymmetric examples are dominated by mononuclear Pt or Ru species, for which it is possible to prepare *trans*-[ArC≡C-(ML$_n$)-Cl] first and subsequently displace the Cl ligand with C≡CAr′.[33] A more exotic approach involves the photolytic activation of *trans*-[ArC≡C-(FeL$_n$)-CH$_3$] in the presence of HC≡CAr′.[35] As demonstrated in our early study,[26] the alkynylation of [Ru$_2$(dmba)$_4$Cl$_2$] does not proceed in a stepwise fashion. The weak-base-assisted "self-assembly" developed here, though seemingly cumbersome, may be suitable for the preparation of the asymmetric bis-alkynyl species from *trans*-[Cl-(ML$_n$)-Cl] compounds that do not undergo stepwise alkynylation.

Molecular structures: Both the symmetric and unsymmetric [(ArC≡C)-Ru$_2$(dmba)$_4$-(C≡CAr′)] compounds are Ru$_2^{III,III}$ species and have a diamagnetic ground state; this facilitates their characterization by ^{1}H NMR spectroscopy. Compounds **1**–**7** are all highly crystalline and molecular structures of **1**, **2**, **4**, **5** and **7** were determined by single-crystal X-ray diffraction techniques. Structural plots of compounds **1**, **2**, **4**, **5** and **7** are shown in Figures 1 and 2, and selected bond lengths and angles are collected in Tables 2 and 3.

Table 2. Selected bond lengths [Å] and angles [°] for molecules **1**, **2**, **4**, and **5**.

	1	**2**	**4**	**5**
Ru1−Ru2	2.4583(3)	2.4405(9)	2.4542(6)	2.4640(7)
Ru1−C1	2.031(8)	1.985(9)	1.988(6)	2.01(1)
Ru2−C3	1.930(7)	1.978(9)	1.992(5)	1.98(2)
Ru1−N1	2.143(7)	1.986(7)	2.099(5)	1.95(1)
Ru1−N3	1.975(7)	2.076(7)	2.015(4)	2.15(1)
Ru1−N5	1.935(9)	2.061(6)	1.989(5)	–
Ru1−N7	2.128(7)	2.035(7)	2.055(5)	–
Ru2−N2	2.045(7)	2.057(7)	1.986(4)	2.09(1)
Ru2−N4	2.104(7)	2.002(7)	2.047(4)	2.03(1)
Ru2−N6	2.104(8)	2.013(7)	2.111(4)	–
Ru2−N8	2.002(7)	2.082(7)	2.011(4)	–
C1−C2	1.12(1)	1.19(1)	1.194(8)	1.19(2)
C3−C4	1.29(1)	1.21(1)	1.194(7)	1.24(2)
Ru2-Ru1-C1	161.7(2)	173.3(3)	168.2(2)	158.1(3)
Ru1-Ru2-C3	158.6(2)	171.9(2)	168.2(2)	162.9(5)
Ru1-C1-C2	178.4(9)	178.8(9)	177.0(6)	168(1)
Ru2-C3-C4	171.0(6)	176.2(8)	175.3(6)	179(2)
Ar−Ar′ dihedral angle	1.7	86.5	89.2	0

Table 3. Selected bond lengths [Å] and angles [°] for molecules **7**.

Molecule A		Molecule B	
Ru1−Ru2	2.4506(6)	Ru3−Ru4	2.4408(7)
Ru1−N1	2.060(4)	Ru3−N11	2.045(4)
Ru1−N3	1.984(5)	Ru3−N13	2.033(5)
Ru1−N5	2.004(4)	Ru3−N15	2.010(4)
Ru1−N7	2.097(5)	Ru3−N17	2.042(5)
Ru2−N2	2.019(4)	Ru4−N12	2.033(4)
Ru2−N4	2.121(5)	Ru4−N14	2.044(5)
Ru2−N6	2.042(4)	Ru4−N16	2.050(4)
Ru2−N8	1.986(4)	Ru4−N18	2.032(5)
Ru1−C1	1.996(6)	Ru3−C57	1.970(6)
Ru2−C3	1.988(5)	Ru4−C59	1.995(6)
C1−C2	1.190(6)	C57−C58	1.169(7)
C3−C4	1.194(6)	C59−C60	1.157(7)
N−O (NO$_2$)	1.163(8)	N−O (NO$_2$)	1.161(7)
N−C (NMe$_2$)	1.409(8)	N−C (NMe$_2$)	1.428(8)
C1-Ru1-Ru2	166.8(2)	C57-Ru3-Ru4	178.1(2)
C3-Ru2-Ru1	166.9(2)	C59-Ru4-Ru3	177.0(2)
Ar−Ar′ dihedral angle	66.7		15.6

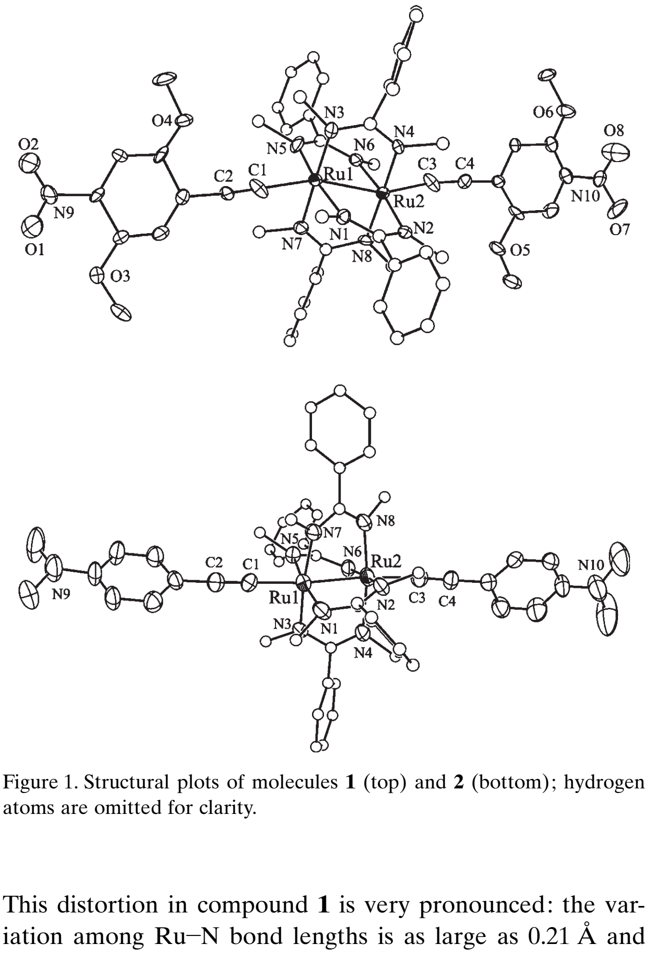

Figure 1. Structural plots of molecules **1** (top) and **2** (bottom); hydrogen atoms are omitted for clarity.

It is clear from Tables 2 and 3 that the Ru−Ru bond lengths in all five compounds are within a narrow range of 2.4405(9)–2.4640(7) Å. These distances are similar to those previously reported for the [Ru$_2$(dmba)$_4$(C≡CY)$_2$]-type compounds (Y = Ar, Fc, SiR$_3$, and C≡CSiR$_3$),[21,23,25–27] and consistent with the existence of a Ru−Ru single bond. The Cα−Cβ bond lengths in all compounds except **1** are very close to 1.20 Å, the value expected for a C≡C bond in metal acetylides.[31,36] A quick glance of structural data of symmetric compounds **1** and **2** reveals that there is a significant structural distortion of the Ru$_2$ coordination sphere from an idealized paddlewheel motif in both compounds (Figure 1). This distortion in compound **1** is very pronounced: the variation among Ru−N bond lengths is as large as 0.21 Å and the Ru−Ru−C bond angle deviates from linearity by about 18°. In comparison, the distortion in compound **2** is more subtle. Such a structural distortion is universal among

Ru_2^{III}–bis-alkynyl complexes,[20,37] and is attributed to a second-order Jahn-Teller effect.[38]

Molecular structures of asymmetric compounds **4**, **5**, and **7** (Figure 2) closely resemble those of the symmetric compounds, especially in terms of geometric parameters associated with the Ru–Ru, Ru–Cα, and Ru–N bonds. These compounds also display notable structural distortions originating from second-order Jahn-Teller effects. One can safely conclude that the donor/acceptor substitution on the phenyl acetylide moiety does not result in a significant structural perturbation in the coordination sphere of Ru_2 unit. Coplanarity of aromatic rings in conjugated molecules such as OPVs (oligo(phenylenevinylene)) and OPEs (oligo(phenyleneethynylene)) is often taken as the structural evidence of extended conjugation.[39] To evaluate the conjugation along ArC≡C-Ru_2-C≡CAr linkage, the dihedral angles between two aryls in *trans*-deposition were calculated and are also listed in Tables 2 and 3. From Table 2 it can be seen that compounds containing 4-NO_2 substituents, namely **1** and **5**, exhibit coplanar conformation, while those containing 4-NMe_2 substituents (**2** and **4**) adopt orthogonal conformation. Intuitively, these conformational preferences appear to be consistent with the electron-rich nature of $\{Ru_2(dmba)_4\}$ core, which transmits hyper-conjugation more readily between electron-poor aromatic rings than between electron-rich ones. However, two crystallographically independent molecules of compound **7** exhibit very different Ar–Ar′ dihedral angles, implying that the observed conformations also depend on crystal-packing forces.

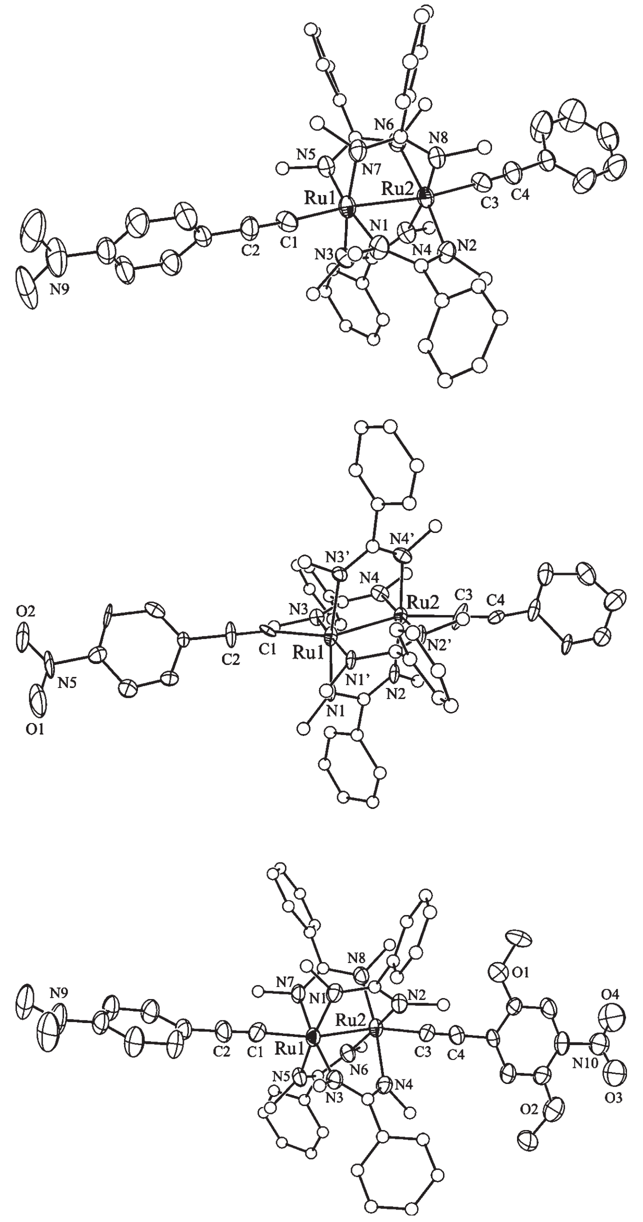

Figure 2. Structural plots of molecules **4** (top), **5** (middle), and **7** (bottom); hydrogen atoms are omitted for clarity.

Electrochemistry: In keeping with the aim of unimolecular rectifier, we are keen to explore the electronic structures of compounds **1**–**7**, especially the asymmetric species, by using voltammetric measurements. Both the cyclic and differential pulse voltammograms (CVs and DPVs) of all compounds, except **6**, were recorded in THF. The DPV plots are provided in Figure 3, and potential data for all observed couples are collected in Table 4 along with those of known compounds $[Ru_2(dmba)_4(C{\equiv}CPh)_2]$ and $[Ru_2(dmba)_4(C{\equiv}CPhNO_2)_2]$ for the purpose of comparison.[25] Similar to the previously studied $[Ru_2(dmba)_4(C{\equiv}CY)_2]$-type compounds,[25–27] all compounds studied here exhibit the Ru_2-based 1 e^- oxidation (**A**) and reduction (**B**), and both are reversible in general. Compared with the symmetric compound $[Ru_2(dmba)_4(C{\equiv}CPh)_2]$, new compounds bearing acceptor substituent on one or both phenylacetylide ligands

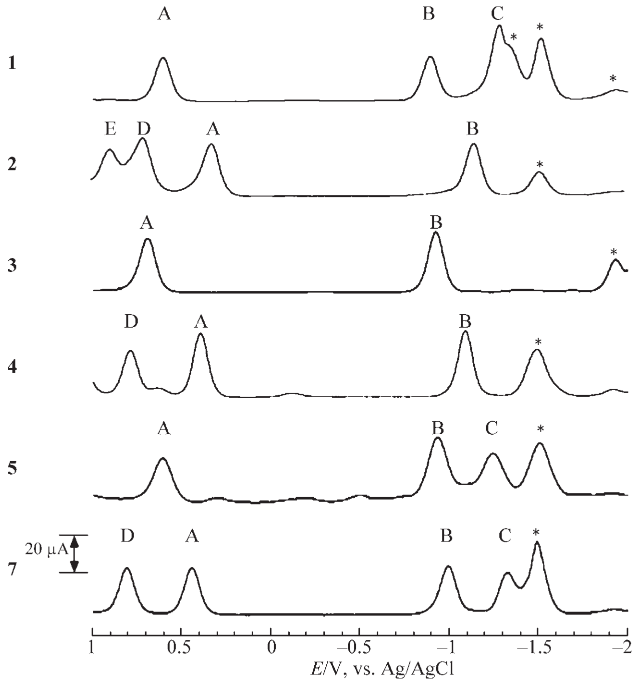

Figure 3. DPVs of compounds **1**–**5** and **7** recorded in THF.

Table 4. Electrode potentials [V] for compounds **1**–**5** and **7**.

	E(**A**)	E(**B**)	E_g[a]	E(**C**)	E(**D**)	E(**E**)	$\Sigma\sigma_X$
1	0.60	−0.89	1.49	−1.28	–	–	1.08
2	0.32	−1.16	1.48	–	0.71	0.90	−1.66
3	0.69	−0.92	1.61	–	–	–	–
4	0.39	−1.10	1.49	–	0.78	–	−0.83
5	0.60	−0.94	1.54	−1.24	–	–	0.81
7	0.44	−1.00	1.44	−1.33	0.81	–	−0.29
$[Ru_2(dmba)_4(C{\equiv}CPh)_2]$[b]	0.52	−1.10	1.62	–	–	–	0
$[Ru_2(dmba)_4(C{\equiv}CPhNO_2)_2]$[b]	0.69	−0.87	1.56	−1.29	–	–	1.62

[a] HOMO–LUMO gap $E_g = E(\mathbf{A}) - E(\mathbf{B})$. [b] Taken from reference [25].

(**1**, **3**, and **5**) display anodically shifted couples, and those bearing donor substituent display cathodically shifted couples (**2** and **4**). The availability of data for both E(**A**) and E(**B**) enables the estimation of HOMO–LUMO gap (E_g) based on the relationship: $E_g = E(\mathbf{A}) - E(\mathbf{B})$,[40,41] and the estimated HOMO–LUMO gaps range from 1.44 to 1.61 V (Table 4).

In addition to the Ru_2-based couples, a number of ligand-center redox couples were also observed in the substituted species. Compound **1** exhibits several reduction couples in the cathodic region beyond the couple **B**, and couple **C** is attributed to the reduction of NO_2. Further reduction results in the degradation of diruthenium species through the dissociation of the acetylide ligand, and the related couples are marked with a "*" in Figure 3. We were perplexed initially to note that the electrode potentials of couples **A**, **B**, and **C** in **1**, a species bearing two 4-NO_2 groups, are very close to those of corresponding couples in **5**, a compound containing only one 4-NO_2 group. Careful perusal of literature revealed that an *ortho*-methoxy group is a moderate electron donor (Hammett constant $\sigma = -0.37$),[42] and its presence partially offsets the electron-withdrawing effect of the 4-NO_2 substituent ($\sigma = 0.81$). Compound **4** exhibits one NMe_2-based oxidation (**D**), while compound **2** displays a stepwise oxidation of NMe_2 substituents (**D** and **E**) indicative of an electronic coupling between two 4-NMe_2 groups across the $[C_6H_4C{\equiv}C\text{-}Ru_2(dmba)_4\text{-}C{\equiv}CC_6H_4]$ fragment. The most attractive of all is the voltammetric behavior of **7**: it displays concurrently an NMe_2 oxidation and a NO_2 reduction in addition to the Ru_2-based **A** and **B** couples.

Prior studies from groups of Lapinte[43,44] and Ren[25] revealed that both the electrode potentials and optical transition energy of {M-C≡C-ArX} species exhibit a linear dependence on the Hammett constant of aryl-substituent X. Electrode potentials for all compounds except **3** were analyzed by the use of the Equation (1) for which the composite Hammett constants $\Sigma\sigma_X$ are also listed in Table 4, and ρ is the reactivity constant.

$$E(\mathrm{X}) = E(\mathrm{H}) + \rho\left(\sum \sigma_\mathrm{X}\right) \quad (1)$$

The resultant plots are shown in Figure 4. The potentials of oxidation couple **A** yield a good linear fit and a stronger substituent dependence ($\rho = 114$ mV), while the potentials of reduction couple **B** yield a less satisfactory fit and a weaker substituent dependence ($\rho = 93$ mV). The reactivity constants estimated herein are in good agreement with those from our early study,[25,38,40,45] but significantly smaller than the constant determined for the oxidation of [Cp*Fe(dppe)(C≡CArX)] (157 mV; dppe = 1,2-bis(diphenylphosphino)ethane),[43] reflecting better conjugation between the metal center and the phenylacetylide ligand in the latter series.

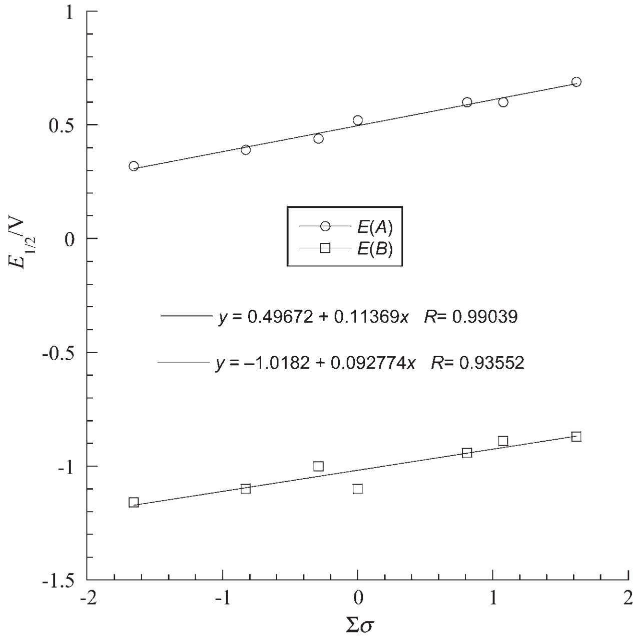

Figure 4. Linear free-energy relationships between the electrode potentials of Ru_2-based couples and the sum of Hammett constants.

Ramification of voltammetric data and future directions: As pointed out in the original proposal of Aviram and Ratner,[1] and numerous subsequent experimental and theoretical studies,[3,46] the key to a significant current rectification is the proper alignment of energy levels within the molecule and with the Fermi levels of both the source and drain electrodes. Hence the underlying question is whether the voltammetric characteristics of unsymmetric compounds qualify D-Ru_2-A species as a prototype of a unimolecular diode. An experimental energy level diagram of compound **7** is shown in Figure 5; it was constructed by aligning orbital energy levels with the peak positions in the DPV of **7** and plotted with a vertical potential scale. When molecules like **7** are sandwiched between a pair of electrodes with the donor-end attached to the source electrode and the acceptor-end to the drain electrode, an electron is injected into the LUMO+1

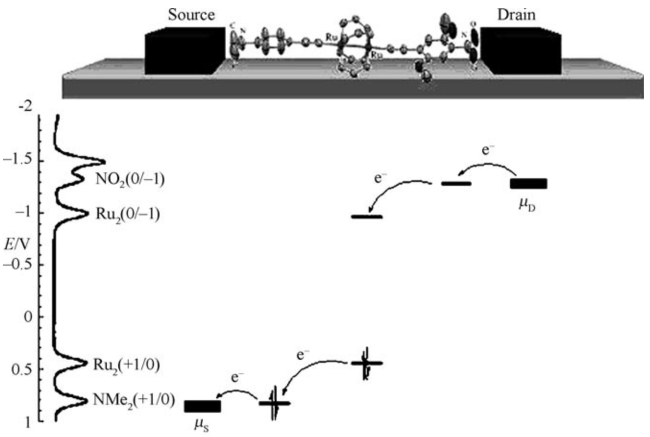

Figure 5. Experimental energy level diagram of compound **7**.

upon matching the electrochemical potential of the drain electrode (μ_D).[47] Further migration of the injected electron through the LUMO, HOMO, and HOMO−1, and to the source electrode completes the current flow of electrons from the drain to the source and is energetically downhill. On the reversal of potential bias, a much higher bias voltage would be required to inject an electron into the lowest occupied MO on 4-NMe_2-C_6H_4. Hence, the current level in the negative bias should remain very low.

Although the D-Ru_2-A compounds reported herein do not conform to the donor–(saturated bridge)–acceptor architecture outlined in the Aviram–Ratner ansatz, the energetic alignment of frontier orbitals does reveal the potential for rectification. We noted that in most of the literature examples of unimolecular rectification, such as thiophene–thiazole diblock oligomers,[5] molecular structures also significantly deviate from the donor–(saturated bridge)–acceptor paradigm. Of course, the Ru_2 compounds reported herein cannot be directly incorporated into nano junctions because of the lack of thiol-capping groups. Currently, we are pursuing analogues of compound **7** with orthogonally protected thiols on both ends. In addition, recent efforts from many groups around the world have resulted in an extended array of diruthenium compounds similar to those reported here.[48] It is possible to realize other types of D-Ru_2-A assembly on the basis of these established examples.

Experimental Section

[$Pd(PPh_3)_2Cl_2$] and 4-ethynylpyridine hydrochloride were purchased from Aldrich; diethylamine, potassium *tert*-butoxide, and PhC≡CH were purchased from ACROS; trimethylsilylacetylene was purchased from GFS, and silica gel was purchased from Merck. [$Ru_2(dmba)_4(NO_3)_2$],[28] 4-$Me_2NC_6H_4C{\equiv}CH$, and 4-$O_2NC_6H_4C{\equiv}CH$ were prepared according to the literature.[30,49] The nitration of 1,5-diiodo-1,4-dimethoxybenzene[50] yielded 4-O_2N-2,5-$(MeO)_2C_6H_4I$,[29] which was converted to 4-O_2N-2,5-$(OMe)_2C_6H_2C{\equiv}CH$ by the Sonogashira reaction.[30,49] THF was distilled over Na/benzophenone under an N_2 atmosphere prior to use. ^1H NMR spectra were recorded on a Bruker AVANCE300 NMR spectrometer. Vis/NIR spectra were obtained with a Perkin–Elmer Lambda-900 UV/Vis/NIR spectrophotometer in THF. Cyclic voltammograms were recorded in 0.2 M (n-Bu)$_4$NPF$_6$ solution on a CHI620 A voltammetric analyzer with a glassy-carbon working electrode (diameter = 2 mm), a Pt-wire auxiliary electrode, and a Ag/AgCl reference electrode. The concentration of diruthenium species was always 1.0 mM. The ferrocenium/ferrocene couple was observed at 0.586 V (vs. Ag/AgCl) under experimental conditions.

Synthesis of [$Ru_2(dmba)_4(C{\equiv}CC_6H_2$-2,5-$(OMe)_2$-4-$NO_2)_2$] (1): 4-$O_2N$-2,5-$(OMe)_2C_6H_2C{\equiv}CH$ (0.136 g, 0.66 mmol), and Et_2NH (20 mL) were added to a suspension of [$Ru_2(dmba)_4(NO_3)_2$] (0.200 g, 0.22 mmol) in THF (70 mL). The reaction mixture was stirred at room temperature for 1 h. Upon the solvent removal, the residue was purified by column chromatography, and eluted with THF/hexanes (1:2, v/v) to afford a reddish solid 0.150 g (56 %). $R_f = 0.50$ (THF/hexanes, 1:2, v/v); ^1H NMR (400 MHz, $CDCl_3$): $\delta = 7.35$–7.33 (m, 15H; aromatic), 6.98 (s, 7H; aromatic), 6.73 (s, 2H; aromatic), 3.74 (s, 6H; CH_3O-), 3.62 (s, 6H; CH_3O-), 3.24 ppm (s, 24H; MeN-); Vis/NIR: λ_{max} (ε) = 819 (2,020), 506 (20,600), 437 nm (17700 $M^{-1}cm^{-1}$); MS-FAB: m/z (%): 1205 [M^++H]; cyclic voltammogram: **A**, $E_{1/2} = 0.566$ V, $\Delta E_p = 0.101$ V, $i_{backward}/i_{forward} = 0.996$; **B**, $E_{1/2} = -0.910$ V, $\Delta E_p = 0.076$ V, $i_{backward}/i_{forward} = 0.866$; elemental analysis calcd (%) for $C_{56}H_{60}N_{10}O_8Ru_2{\cdot}H_2O$ (1221.29): C 55.07, H 5.12, N 11.47; found C 54.66, H 4.91, N 11.42.

Synthesis of [$Ru_2(dmba)_4(C{\equiv}CC_6H_4$-4-$NMe_2)_2$] (2): 4-$Me_2NC_6H_4C{\equiv}CH$ (0.096 g, 0.66 mmol), and Et_2NH (20 mL) were added to a suspension of [$Ru_2(dmba)_4(NO_3)_2$] (0.200 g, 0.22 mmol) in THF (60 mL). The reaction mixture was stirred at room temperature for 2 h. Upon the solvent removal, the residue was purified by column chromatography, and eluted with THF/hexanes (1:2, v/v) to afford a reddish solid 0.130 g (55 %). The sample was authenticated by comparison of the R_f value (0.75 in THF/hexanes, 1:2, v/v) with literature.[25]

Synthesis of [$Ru_2(dmba)_4(C{\equiv}C$-4-$C_5H_4N)_2$] (3): A mixture of [$Ru_2(dmba)_4(NO_3)_2$] (0.300 g, 0.32 mmol), 4-ethynylpyridine hydrochloride (0.137 g, 0.98 mmol), and potassium *tert*-butoxide (0.110 g, 0.98 mmol) in THF (200 mL) was stirred under argon at room temperature overnight. The reaction mixture changed from dark green to dark red during the process of the reaction. Use of Et_2NH (10 mL) in place of potassium *tert*-butoxide gave the same result. The reaction mixture was filtered through a plug of silica gel. Upon the solvent removal, the residue was purified by recrystallization from THF and hexane to obtain reddish solid 0.240 g (75 %). $R_f = 0.60$ (THF/hexanes, 1:1, v/v); ^1H NMR (300 MHz, $CDCl_3$): $\delta = 8.30$ (d, $J = 6$ Hz, 4H; aromatic), 7.44–7.38 (m, 12H; aromatic), 6.90 (d, $J = 14$ Hz, 8H; aromatic), 6.88 (d, $J = 14$ Hz, 4H; aromatic), 3.24 ppm (s, 24H; MeN-); Vis/NIR: λ_{max} (ε) = 839 (2320), 500 nm (9990 $M^{-1}cm^{-1}$); MS-FAB: m/z (%): 997 [M^++H]; cyclic voltammogram: **A**, $E_{1/2} = 0.616$ V, $\Delta E_p = 0.056$ V, $i_{backward}/i_{forward} = 0.687$; **B**, $E_{1/2} = -0.996$ V, $\Delta E_p = 0.063$ V, $i_{backward}/i_{forward} = 0.950$; elemental analysis calcd (%) for $C_{50}H_{52}N_{10}Ru_2{\cdot}H_2O$ (1013.17): C 59.27, H 5.37, N 13.82; found: C 59.75, H 5.43, N 13.62.

Synthesis of [(4-$Me_2NC_6H_4C{\equiv}C$)$Ru_2(dmba)_4(C{\equiv}CC_6H_5)$] (4): To a suspension of $Ru_2(dmba)_4(NO_3)_2$ (0.183 g, 0.20 mmol) and THF (60 mL) was added a THF solution containing a mixture of 4-$Me_2NC_6H_4C{\equiv}CH$ (0.073 g, 0.60 mmol), $C_6H_5C{\equiv}CH$ (0.022 mL, 0.20 mmol) and Et_2NH (20 mL). The reaction was stirred at room temperature and the progress of the reaction was monitored by TLC. Upon the completion of the reaction, the solvent was removed. The residue was purified by column chromatography and eluted with THF/hexanes (1:3, v/v) to yield a trace amount of **2**, 0.065 g of **4** (30 % based on Ru), and 0.060 g of [$Ru_2(dmba)_4(C{\equiv}CC_6H_5)_2$] (30 % based on Ru). Data for **4**: $R_f = 0.66$ (THF/hexanes, 1:2, v/v); ^1H NMR (400 MHz, $CDCl_3$): $\delta = 7.47$–7.39 (m, 12H; aromatic), 7.18–7.12 (m, 5H; aromatic), 7.06–7.02 (m, 10H; aromatic), 6.61 (d, $J = 9$ Hz, 2H; aromatic), 3.31 (d, $J = 1$ Hz, 24H; MeN-), 2.89 ppm (s, 6H; MeN-); Vis/NIR: λ_{max} (ε) = 892 (1830), 502 (12300), 394 nm (7370 $M^{-1}cm^{-1}$); MS-FAB: m/z (%): 1038 [M^++H]; cyclic voltammogram: **A**, $E_{1/2} = 0.372$ V, $\Delta E_p = 0.061$ V, $i_{backward}/i_{forward} = 0.706$; **B**, $E_{1/2} = -1.117$ V, $\Delta E_p = 0.061$ V, $i_{backward}/i_{forward} = 0.471$; elemental analysis calcd

(%) for $C_{54}H_{59}N_9Ru_2{\cdot}THF{\cdot}2\,H_2O$ (1144.38): C 60.87, H 6.25, N 11.02; found: C 60.64, H 6.02, N 10.81.

Synthesis of [$(C_6H_5C{\equiv}C)Ru_2(dmba)_4(C{\equiv}CC_6H_4$-4-$NO_2$)] (5): A solution of 4-$O_2NC_6H_4C{\equiv}CH$ (0.029 g, 0.20 mmol), $C_6H_5C{\equiv}CH$ (0.055 mL, 0.50 mmol), and Et_2NH (20 mL) in THF (60 mL) was added to a suspension of [$Ru_2(dmba)_4(NO_3)_2$] (0.183 g, 0.20 mmol) and THF (60 mL). The mixture was stirred at room temperature and the progress of the reaction was monitored by TLC. Upon the completion of the reaction, the solvent was removed. The residue was purified by column chromatography and eluted with EtOAC/hexanes (1:5, v/v) to yield 0.020 g of [$Ru_2(dmba)_4(C{\equiv}CC_6H_5)_2$] (10 % based on Ru), 0.070 g of **5** (34 % based on Ru), and 0.060 g of [$Ru_2(dmba)_4(C{\equiv}CC_6H_4$-4-$NO_2)_2$] (28 % based on Ru). Data for **5**: $R_f=0.40$ (EtOAc/hexanes, 1:2, v/v); ^1H NMR (400 MHz, $CDCl_3$): $\delta=8.05$ (d, $J=9$ Hz, 2H; aromatic), 8.49–8.41 (m, 12H; aromatic), 7.15 (d, $J=7$ Hz, 6H; aromatic), 7.03–7.699 (m, 9H; aromatic), 3.29 ppm (s, 24H; MeN-); Vis/NIR: λ_{max} (ε) = 877 (2680), 510 (28 800), 460 (27 400), 426 nm (24 100 $M^{-1}cm^{-1}$); MS-FAB: m/z (%): 1040 [M^++H]; cyclic voltammogram: **A**, $E_{1/2}=0.570$ V, $\Delta E_p=0.114$ V, $i_{backward}/i_{forward}=0.286$; **B**, $E_{1/2}=-0.966$ V, $\Delta E_p=0.110$ V, $i_{backward}/i_{forward}=0.374$; elemental analysis calcd (%) for $C_{52}H_{53}N_9O_2Ru_2{\cdot}1.5\,H_2O{\cdot}EtOAc$ (1153.30): C 58.32, H 5.59, N 10.93; found: C 58.71, H 5.57, N 10.45.

Synthesis of [(4-$Me_2NC_6H_4C{\equiv}C)Ru_2(dmba)_4(C{\equiv}CC_6H_4$-4-$NO_2$)] (6): A solution of 4-$Me_2NC_6H_4C{\equiv}CH$ (0.073 g, 0.60 mmol), 4-$O_2NC_6H_2C{\equiv}CH$ (0.029 g, 0.20 mmol), and Et_2NH (20 mL) in THF (80 mL) was added to a suspension of [$Ru_2(dmba)_4(NO_3)_2$] (0.183 g, 0.20 mmol) and THF (60 mL). The mixture was stirred at room temperature and the progress of the reaction was monitored by TLC. The reaction was stirred at room temperature for an hour, and TLC analysis indicated the consumption of the starting material and also the following distribution of the products: trace amount of compound **2** (($R_f=0.75$ in THF/hexanes, 1:2, v/v), 40 % of compound **6** ($R_f=0.70$), and 40 % of [$Ru_2(dmba)_4(C{\equiv}CC_6H_4$-4-$NO_2)_2$] ($R_f=0.65$). Attempted separation of the three products failed due to both the poor solubility and similar polarity of three compounds ($R_f=0.70$ for compound **6**, 0.65 for [$Ru_2(dmba)_4(C{\equiv}CC_6H_4$-4-$NO_2)_2$], and 0.70 for compound **2** in THF/hexanes, 1:2, v/v).

Synthesis of [(4-$Me_2NC_6H_4C{\equiv}C)Ru_2(dmba)_4(C{\equiv}CC_6H_2$-2,5-$(OMe)_2$-4-$NO_2$)] (7): A solution of 4-$Me_2NC_6H_4C{\equiv}CH$ (0.044 g, 0.30 mmol), 4-O_2N-2,5-$(OMe)_2C_6H_2C{\equiv}CH$ (0.020 g, 0.10 mmol), and Et_2NH (20 mL) in THF (50 mL) was added to a suspension of [$Ru_2(dmba)_4(NO_3)_2$] (0.092 g, 0.10 mmol) and THF (60 mL). The mixture was stirred at room temperature and the progress of the reaction was monitored by TLC. Upon the solvent removal, the residue was purified by column chromatography, and eluted with EtOAc/hexanes (1:5, v/v) to afford a trace amount of compound **2**, 0.030 g of compound **7** (26 % based on Ru), and 0.030 g of compound **1** (27 % based on Ru). Data for **7**: $R_f=0.62$ (EtOAc/hexanes, 1:2, v/v); ^1H NMR (300 MHz, $CDCl_3$): $\delta=7.35$–7.33 (m, 13H; aromatic), 7.08–7.02 (m, 10H; aromatic), 6.75 (s, 1H; aromatic), 6.64 (d, $J=7$ Hz, 2H; aromatic), 3.85 (s, 3H; CH_3O-), 3.73 (s, 3H; CH_3O-), 3.00 (s, 24H; MeN-), 2.82 ppm (s, 6H; MeN-); Vis/NIR: λ_{max} (ε) = 883 (2080), 510 (24 500), 427 nm (18 400 $M^{-1}cm^{-1}$) nm; MS-FAB: m/z (%): 1142 [M^++H]; cyclic voltammogram: **A**, $E_{1/2}=0.415$ V, $\Delta E_p=0.059$ V, $i_{backward}/i_{forward}=0.878$; **B**, $E_{1/2}=-1.015$ V, $\Delta E_p=0.072$ V, $i_{backward}/i_{forward}=0.577$; elemental analysis calcd (%) for $C_{56}H_{62}N_{10}O_4Ru_2{\cdot}3\,EtOAc$ (1405.61): C 58.10, H 6.17, N 9.96; found C 58.16, H 6.17, N 9.56.

Structure determination: Single crystals were obtained by slow evaporation of solutions of **1** or **2** in hexanes/THF, by evaporation of a solution of **4** in hexanes/ethyl acetate, and by slow diffusion of hexanes into a solution of **5** in benzene or **7** in toluene/THF. X-ray intensity data were measured at 300 K on a Bruker SMART1000 CCD-based X-ray diffractometer system with $Mo_{K\alpha}$ radiation ($\lambda=0.71073$ Å). Data were measured by omega scans of 0.3° per frame such that a hemisphere (1271 frames) was collected. The frames were integrated with the Bruker SAINT software package[51] by using a narrow-frame integration algorithm, which also corrects for the Lorentz and polarization effects. Absorption corrections were applied with SADABS. Structures were solved and refined with the Bruker SHELXTL (Version 5.1) software package.[52] The positions of all non-hydrogen atoms were revealed by direct methods. All non-hydrogen atoms are refined anisotropically and the hydrogen atoms were put in calculated positions and riding mode. Each structure was refined to convergence by least squares method on F^2, SHELXL-93, incorporated in SHELXTL.PC V 5.03. Crystallographic data are given in Table 5. CCDC-642082–642086 (for compounds **1**, **2**, **4**, **5**, and **7**, respectively) contain the supplementary crystallographic data for this paper. These data can be obtained free of charge from The Cambridge Crystallographic Data Centre viawww.ccdc.cam.ac.uk/data_request/cif.

Table 5. Crystallographic data for compounds **1**, **2**, **4**, **5**, and **7**.

	1·4THF	**2**	**4**	**5**·3 C_6H_6	**7**·0.5THF
formula	$C_{72}H_{92}N_{10}O_{12}Ru_2$	$C_{56}H_{64}N_{10}Ru_2$	$C_{54}H_{59}N_9Ru_2$	$C_{70}H_{71}N_9O_2Ru_2$	$C_{58}H_{62}N_{10}O_{4.5}Ru_2$
M_r	1491.7	1079.31	1036.24	1272.5	1173.32
T [K]	300(2)	300(2)	300(2)	300(2)	300(2)
crystal system	triclinic	monoclinic	monoclinic	monoclinic	triclinic
space group	$P1$	$P2_1/n$	$P2_1/n$	Cm	$P\bar{1}$
crystal dimensions [mm]	0.36 × 0.27 × 0.10	0.24 × 0.10 × 0.02	0.43 × 0.41 × 0.03	0.39 × 0.36 × 0.04	0.47 × 0.23 × 0.05
a [Å]	12.1538(5)	12.0797(7)	10.0612(5)	11.4214(7)	14.8241(6)
b [Å]	12.9209(6)	17.673(1)	46.289(2)	18.692(1)	20.7087(9)
c [Å]	13.2864(6)	28.057(2)	11.6366(6)	15.607(1)	21.8769(9)
α [°]	91.826(1)				68.589(1)
β [°]	98.977(1)	98.693(1)	110.021(1)	105.648(1)	78.475(1)
γ [°]	114.853(1)				71.275(1)
V [Å^3]/Z	1859.0(1)	5920.8(6)	5091.9(5)	3208.3(4)	5895.5(4)
Z	1	4	4	2	4
ρ_{calcd} [g cm^{-3}]	1.332	1.211	1.352	1.317	1.322
μ [mm^{-1}]	0.471	0.551	0.637	0.522	0.565
θ range [°]	1.75–25.00	1.75–25.00	1.76–25.00	2.15–24.99	1.69–25.00
reflections measured	9861	30 661	26 727	8440	31 565
unique reflections (R_{int})	7905 (0.012)	10 437 (0.109)	8943 (0.054)	5037 (0.029)	20 551 (0.034)
data/restraints/parameters	7905/3/824	10 437/0/613	8943/0/586	5037/2/395	20 551/0/1317
goodness-of-fit on F^2	1.02	1.01	1.00	1.01	1.01
final R indices [$I>2\sigma(I)$]	$R_1=0.029/wR_2=0.069$	$R_1=0.069/wR_2=0.172$	$R_1=0.058/wR_{2=}0.122$	$R_1=0.037/wR_2=0.082$	$R_1=0.049/wR_2=0.096$
R indices (all data)	$R_1=0.039/wR_2=0.072$	$R_1=0.165/wR_2=0.204$	$R_1=0.102/wR_2=0.137$	$R_1=0.056/wR_2=0.087$	$R_1=0.133/wR_2=0.113$
max/min $\Delta\rho$ [e Å^{-3}]	0.39/−0.33	1.15/−0.40	0.39/−0.37	1.17/−0.37	0.68/−0.35

Acknowledgements

We are grateful to the National Science Foundation (CHE0242623/0553564 and CHE0715404) and Purdue University for providing financial support.

---

[1] A. Aviram, M. A. Ratner, *Chem. Phys. Lett.* **1974**, *29*, 277–283.

[2] *Molecular Nanoelectronics* (Eds.: M. A. Reed, T. Lee), American Scientific, Stevenson Ranch, CA, **2003**.

[3] R. M. Metzger, *Chem. Rev.* **2003**, *103*, 3803–3834; G. Ho, J. R. Heath, M. Kondratenko, D. F. Perepichka, K. Arseneault, M. Pézolet, M. R. Bryce, *Chem. Eur. J.* **2005**, *11*, 2914–2922.

[4] G. J. Ashwell, W. D. Tyrrell, A. J. Whittam, *J. Am. Chem. Soc.* **2004**, *126*, 7102–7110.

[5] M. K. Ng, D. C. Lee, L. P. Yu, *J. Am. Chem. Soc.* **2002**, *124*, 11862–11863; M. K. Ng, L. P. Yu, *Angew. Chem.* **2002**, *114*, 3750–3753; *Angew. Chem. Int. Ed.* **2002**, *41*, 3598–3601; P. Jiang, G. M. Morales, W. You, L. P. Yu, *Angew. Chem. Int. Ed.* **2004**, *116*, 4571–4574; *Angew. Chem. Int. Ed.* **2004**, *43*, 4471–4475; G. M. Morales, P. Jiang, S. W. Yuan, Y. G. Lee, A. Sanchez, W. You, L. P. Yu, *J. Am. Chem. Soc.* **2005**, *127*, 10456–10457.

[6] J. Zhao, C. G. Zeng, X. Cheng, K. D. Wang, G. W. Wang, J. L. Yang, J. G. Hou, Q. S. Zhu, *Phys. Rev. Lett.* **2005**, *95*, 045502.

[7] F. Jackel, M. D. Watson, K. Müllen, J. P. Rabe, *Phys. Rev. Lett.* **2004**, *92*, 188303.

[8] M. Elbing, R. Ochs, M. Koentopp, M. Fischer, C. von Hanisch, F. Weigend, F. Evers, H. B. Weber, M. Mayor, *Proc. Natl. Acad. Sci. USA* **2005**, *102*, 8815–8820.

[9] F. Paul, C. Lapinte, *Coord. Chem. Rev.* **1998**, *178–180*, 431–509.

[10] F. Paul, C. Lapinte in *Unusual Structures and Physical Properties in Organometallic Chemistry* (Eds.: M. Gielen, R. Willem, B. Wrackmeyer), Wiley, Chichester, **2002**.

[11] J. Park, A. N. Pasupathy, J. L. Goldsmith, C. Chang, Y. Yaish, J. R. Petta, M. Rinkoski, J. P. Sethna, H. D. Abruna, P. L. McEuen, D. C. Ralph, *Nature* **2002**, *417*, 722–725.

[12] W. J. Liang, M. P. Shores, M. Bockrath, J. R. Long, H. Park, *Nature* **2002**, *417*, 725–729.

[13] D.-H. Chae, J. F. Berry, S. Jung, F. A. Cotton, C. A. Murillo, Z. Yao, *Nano Lett.* **2006**, *6*, 165–168.

[14] F. Coat, C. Lapinte, *Organometallics* **1996**, *15*, 477–479.

[15] R. Dembinski, T. Bartik, B. Bartik, M. Jaeger, J. A. Gladysz, *J. Am. Chem. Soc.* **2000**, *122*, 810–822; M. Brady, W. Weng, Y. Zou, J. W. Seyler, A. J. Amoroso, A. M. Arif, M. Bohme, G. Frenking, J. A. Gladysz, *J. Am. Chem. Soc.* **1997**, *119*, 775–788.

[16] F. Paul, W. E. Meyer, L. Toupet, H. Jiao, J. A. Gladysz, C. Lapinte, *J. Am. Chem. Soc.* **2000**, *122*, 9405–9414.

[17] K. Venkatesan, O. Blacque, H. Berke, *Dalton Trans.* **2007**, 1091–1100.

[18] M. I. Bruce, P. J. Low, K. Costuas, J.-F. Halet, S. P. Best, G. A. Heath, *J. Am. Chem. Soc.* **2000**, *122*, 1949–1962; M. I. Bruce, B. G. Ellis, P. J. Low, B. W. Skelton, A. H. White, *Organometallics* **2003**, *22*, 3184–3198; L.-B. Gao, L.-Y. Zhang, L.-X. Shi, Z.-N. Chen, *Organometallics* **2005**, *24*, 1678–1684; S. Rigaut, C. Olivier, K. Costuas, S. Choua, O. Fadhel, J. Massue, P. Turek, J.-Y. Saillard, P. H. Dixneuf, D. Touchard, *J. Am. Chem. Soc.* **2006**, *128*, 5859–5876.

[19] S. A. Getty, C. Engtrakul, L. Wang, R. Liu, S.-H. Ke, H. U. Baranger, W. Yang, M. S. Fuhrer, L. R. Sita, *Phys. Rev. B* **2005**, *71*, No. 241401.

[20] T. Ren, *Organometallics* **2005**, *24*, 4854–4870.

[21] G.-L. Xu, R. J. Crutchley, M. C. DeRosa, Q.-J. Pan, H.-X. Zhang, X. Wang, T. Ren, *J. Am. Chem. Soc.* **2005**, *127*, 13354–13363.

[22] Y. Shi, G. T. Yee, G. Wang, T. Ren, *J. Am. Chem. Soc.* **2004**, *126*, 10552–10553; G.-L. Xu, G. Zou, Y.-H. Ni, M. C. DeRosa, R. J. Crutchley, T. Ren, *J. Am. Chem. Soc.* **2003**, *125*, 10057–10065.

[23] G.-L. Xu, M. C. DeRosa, R. J. Crutchley, T. Ren, *J. Am. Chem. Soc.* **2004**, *126*, 3728–3729.

[24] A. S. Blum, T. Ren, D. A. Parish, S. A. Trammell, M. H. Moore, J. G. Kushmerick, G.-L. Xu, J. R. Deschamps, S. K. Pollack, R. Shashidhar, *J. Am. Chem. Soc.* **2005**, *127*, 10010–10011.

[25] S. K. Hurst, G.-L. Xu, T. Ren, *Organometallics* **2003**, *22*, 4118–4123.

[26] G.-L. Xu, C. Campana, T. Ren, *Inorg. Chem.* **2002**, *41*, 3521–3527.

[27] G.-L. Xu, C. G. Jablonski, T. Ren, *J. Organomet. Chem.* **2003**, *683*, 388–397.

[28] G.-L. Xu, C. G. Jablonski, T. Ren, *Inorg. Chim. Acta* **2003**, *343*, 387–390.

[29] G. M. Robinson, *J. Chem. Soc. Trans* **1916**, *109*, 1078–1091.

[30] K. Sonogashira, Y. Tohda, N. Hagihara, *Tetrahedron Lett.* **1975**, *16*, 4467–4470.

[31] M. I. Bruce, P. J. Low, *Adv. Organomet. Chem.* **2004**, *50*, 179–444.

[32] N. J. Long, C. K. Williams, *Angew. Chem.* **2003**, *115*, 2690–2722; *Angew. Chem. Int. Ed.* **2003**, *42*, 2586–2617.

[33] A. M. McDonagh, M. P. Cifuentes, I. R. Whittall, M. G. Humphrey, M. Samoc, B. Luther-Davies, D. C. R. Hockless, *J. Organomet. Chem.* **1996**, *526*, 99–103; M. Younus, N. J. Long, P. R. Raithby, J. Lewis, N. A. Page, A. J. P. White, D. J. Williams, M. C. B. Colbert, A. J. Hodge, M. S. Khan, D. G. Parker, *J. Organomet. Chem.* **1999**, *578*, 198–209; K. Onitsuka, M. Fujimoto, N. Ohshiro, S. Takahashi, *Angew. Chem.* **1999**, *111*, 751–754; *Angew. Chem. Int. Ed.* **1999**, *38*, 689–692; R. D'Amato, A. Furlani, M. Colapietro, G. Portalone, M. Casalboni, M. Falconieri, M. V. Russo, *J. Organomet. Chem.* **2001**, *627*, 13–22; C. Desroches, C. Lopes, V. Kessler, S. Parola, *Dalton Trans.* **2003**, 2085–2092; C.-H. Tao, N. Zhu, V. W.-W. Yam, *Chem. Eur. J.* **2005**, *11*, 1647–1657; X. Zhao, T. Cardolaccia, R. T. Farley, K. A. Abboud, K. S. Schanze, *Inorg. Chem.* **2005**, *44*, 2619–2627; C. J. Adams, L. E. Bowen, *Dalton Trans.* **2005**, 2239–2240.

[34] V. W. W. Yam, W. K. M. Fung, K. K. Cheung, *Organometallics* **1998**, *17*, 3293–3298.

[35] L. D. Field, A. J. Turnbull, P. Turner, *J. Am. Chem. Soc.* **2002**, *124*, 3692–3702.

[36] P. J. Low, M. I. Bruce, *Adv. Organomet. Chem.* **2001**, *48*, 71–288; S. Szafert, J. A. Gladysz, *Chem. Rev.* **2006**, *106*, 1–33; S. Szafert, J. A. Gladysz, *Chem. Rev.* **2003**, *103*, 4175–4206.

[37] J. L. Bear, B. Han, S. Huang, K. M. Kadish, *Inorg. Chem.* **1996**, *35*, 3012–3021; S. K. Hurst, T. Ren, *J. Organomet. Chem.* **2003**, *670*, 188–197; T. Ren, G.-L. Xu, *Comments Inorg. Chem.* **2002**, *23*, 355–380.

[38] C. Lin, T. Ren, E. J. Valente, J. D. Zubkowski, *J. Chem. Soc. Dalton Trans.* **1998**, 571–576.

[39] R. E. Martin, F. Diederich, *Angew. Chem.* **1999**, *111*, 1440–1469; *Angew. Chem. Int. Ed.* **1999**, *38*, 1350–1377.

[40] T. Ren, *Coord. Chem. Rev.* **1998**, *175*, 43–58.

[41] R. O. Loutfy, R. O. Loutfy, *Can. J. Chem.* **1976**, *54*, 1454–1463.

[42] M. T. Tribble, J. G. Traynham, *J. Am. Chem. Soc.* **1969**, *91*, 379–388; P. Mamalis, H. N. Rydon, *J. Chem. Soc.* **1955**, 1049–1065.

[43] K. Costuas, F. Paul, L. Toupet, J.-F. Halet, C. Lapinte, *Organometallics* **2004**, *23*, 2053–2068.

[44] F. Paul, G. d. Costa, A. Bondon, N. Gauthier, S. Sinbandhit, L. Toupet, K. Costuas, J.-F. Halet, C. Lapinte, *Organometallics* **2007**, *26*, 874–896.

[45] C. Lin, J. D. Protasiewicz, E. T. Smith, T. Ren, *J. Chem. Soc. Chem. Commun.* **1995**, 2257–2258; C. Lin, J. D. Protasiewicz, T. Ren, *Inorg. Chem.* **1996**, *35*, 7455–7458; C. Lin, J. D. Protasiewicz, E. T. Smith, T. Ren, *Inorg. Chem.* **1996**, *35*, 6422–6428; C. Lin, T. Ren, E. J. Valente, J. D. Zubkowski, E. T. Smith, *Chem. Lett.* **1997**, 753–754; T. Ren, C. Lin, E. J. Valente, J. D. Zubkowski, *Inorg. Chim. Acta* **2000**, *297*, 283–290; C. Lin, T. Ren, E. J. Valente, J. D. Zubkowski, *J. Organomet. Chem.* **1999**, *579*, 114–121.

[46] C. Krzeminski, C. Delerue, G. Allan, D. Vuillaume, R. M. Metzger, *Phys. Rev. B* **2001**, *64*, 085405; K. Stokbro, J. Taylor, M. Brandbyge, *J. Am. Chem. Soc.* **2003**, *125*, 3674–3675.

[47] M. Paulsson, F. Zahid, S. Datta in *Handbook of Nanoscience, Engineering, and Technology* (Ed.: W. A. Goddard), CRC, Boca Raton, **2003**.

[48] J.-L. Zuo, F. F. d. Biani, A. M. Santos, K. Köhler, F. E. Kühn, *Eur. J. Inorg. Chem.* **2003**, 449–452; J.-L. Zuo, E. Herdtweck, F. E. Kühn, *J.*

Chem. Soc. Dalton Trans. **2002**, 1244–1246; M. C. Barral, S. Herrero, R. Jiménez-Aparicio, M. R. Torres, F. A. Urbanos, *Angew. Chem.* **2005**, *117*, 309–311; *Angew. Chem. Int. Ed.* **2005**, *44*, 305–307; D. Olea, R. González-Prieto, J. L. Priego, M. C. Barral, P. J. d. Pablo, M. R. Torres, J. Gómez-Herrero, R. Jiménez-Aparicio, F. Zamora, *Chem. Commun.* **2007**, 1591–1593; T. E. Vos, Y. Liao, W. W. Shum, J.-H. Her, P. W. Stephens, W. M. Reiff, J. S. Miller, *J. Am. Chem. Soc.* **2004**, *126*, 11630–11639; T. E. Vos, J. S. Miller, *Angew. Chem.* **2005**, *117*, 2468–2471; *Angew. Chem. Int. Ed.* **2005**, *44*, 2416–2419; Y. Liao, W. W. Shum, J. S. Miller, *J. Am. Chem. Soc.* **2002**, *124*, 9336–9337.

[49] S. Takahashi, Y. Kuriyama, K. Sonogashira, N. Hagihara, *Synthesis* **1980**, 627–630.

[50] C. J. Yu, Y. C. Chong, J. F. Kayyem, M. Gozin, *J. Org. Chem.* **1999**, *64*, 2070–2079.

[51] SAINT V 6.035 Software for the CCD Detector System, Bruker-AXS Inc., **1999**.

[52] SHELXTL 5.03 (WINDOW-NT Version), Program library for Structure Solution and Molecular Graphics, Bruker-AXS Inc., **1998**.

Received: April 29, 2007